



Palaeoenvironmental reconstruction of an urban archaeological site: the case of the Roman salt mines of Vigo (NW Iberia)

Journal:	<i>Geoarchaeology</i>
Manuscript ID	Draft
Wiley - Manuscript type:	Research Article
Date Submitted by the Author:	n/a
Complete List of Authors:	Armada, Rebeca; Universidade de Santiago de Compostela, Edafoloxía e Química Agrícola Costa-Casais, Manuela; Universidade de Santiago de Compostela, Xeografía Blanco-Chao, Ramón; Universidade de Santiago de Compostela, Xeografía Taboada Rodríguez, Teresa; Universidade de Santiago de Compostela, Edafoloxía e Química Agrícola Martínez Cortizas, Antonio; Universidade de Santiago de Compostela, Edafoloxía e Química Agrícola
Keywords:	Urban Geoarchaeology, coastal evolution, Roman Period, salt mines, NW Spain

SCHOLARONE™
Manuscripts

ew

Palaeoenvironmental reconstruction of an urban archaeological site: the case of the Roman salt mines of Vigo (NW Iberia)

Tallón Armada, Rebeca^{1,*}; Costa-Casais, Manuela²; Blanco-Chao, Ramón²; Taboada Rodríguez, Teresa¹; Martínez Cortizas, Antonio¹

¹ Departamento de Edafología e Química Agrícola, Facultade de Bioloxía, Universidade de Santiago de Compostela (USC), Rúa Lope Gómez de Marzoa, s/n. Campus Vida. 15782 Santiago de Compostela, A Coruña, (Spain). rebeca.tallon@usc.es, teresa.taboada@usc.es, antonio.martinez.cortizas@usc.es

² Departamento de Xeografía, Facultade de Xeografía e Historia, Universidade de Santiago de Compostela (USC). Praza da Universidade 1, 15782, Santiago de Compostela, A Coruña, (Spain). manuela.costa@usc.es, ramon.blanco@usc.es

ABSTRACT

The application of Geoscience to Archaeology has provided a great deal of information about sites related to human activities and their environmental context. The knowledge and techniques that geoarchaeological studies provide are very useful to interpret the complexity of urban areas and their environment. In this article we present the case of the Roman salt mines found in the city of Vigo (NW Spain). From a geoarchaeological approach, we explain their evolution related to the city and its coastline. We integrate pedo-sedimentary, coastal morphodynamic and archaeological information. The results show an evolution from a peri-urban to an urban location. Museumization of the site increased its value for the city, making it part of its cultural heritage. At the same time, the associated pedo-sedimentary deposits should also be considered as part of this (geological) heritage in that they are records which provide essential information regarding the environment and human activity, which enables us to understand and recognise the past. Therefore, in archaeological excavations in urban areas, geoarchaeological work should be considered essential as far as the historical interpretation of the city in question is concerned.

Keywords: Urban Geoarchaeology; coastal evolution; Roman Period; salt mines; NW Spain

1. INTRODUCTION

The constant evolution of cities more or less guarantees the fact that they host a multitude of archaeological remains (be they of urban origin or not), which, over the course of time, may become features of the modern-day city, provided that they are adequately looked after. This is the case of the Roman salt mine of “O Areal” uncovered in the city of Vigo (in the province of Pontevedra, Spain) during the course of public construction works. Their exceptionality and importance in the industry of the age (Curras, 2007) has led to them being converted into a museum and becoming an integral part of the environment of the city (they are located on layer -1 of the building occupied by Sergas, the regional health ministry) (Castro, 2007). They were not originally located in an urban setting but today, due to the growth of the city, they lie within its urban nucleus.

Geoarchaeology applies knowledge and techniques originating from different Earth Science disciplines in order to resolve historico-archaeological problems (Butzer, 1982;

1
2
3 Bennedetti, Cordova, & Beach, 2010; Nicoll & Murphy, 2014; Panin & Bronnikova,
4 2014; Canti Dirk & Huisman, 2015) and is directly linked with paleo-environmental
5 reconstruction in archaeological and environmental archaeological contexts (Dincauze,
6 2000). One of the main focuses of attention of Geoarchaeology is the study of urban
7 sectors as their environment may contain a high degree of complexity in comparison
8 with settlements of a more rural nature (Rothschild & Zerega, 2008). Indeed, these
9 types of applications can be highly informative for urban processes, demographic
10 cycles, or the intersection between sites and their surrounding landscapes (Butzer,
11 2008). This can be seen in the growing number of research projects being carried out in
12 the fields of Urban Archaeology and the Earth Sciences (Shahack-Gross et al 2005;
13 Schuldenrein & Aiuvalasit, 2011; Butzer, Butzer & Love, 2013; Bini et al, 2015; Quirós
14 et al, 2014)

15
16
17 In Galicia (NW Spain) studies of this kind have been going on for several years within
18 our research group (Tallón Armada, 2012; Tallón Armada et al, 2013), in collaboration
19 with specialists in Archaeology, highlighting the importance of carrying out these
20 studies in order to understand the complexity of urban areas. This article has been
21 developed along these lines.
22

23
24 This research aims to study the pedo-sedimentary record of Vigo's salt mine, now
25 converted into a museum, as a methodological application of paleo-environmental
26 reconstruction in archaeological contexts with the ultimate goal of contextualizing and
27 providing an evolutionary framework for the archaeological information displayed in
28 the museum. In order to achieve these aims, it is necessary to analyse the soil and its
29 sediments in terms of stratigraphy, physical and chemical properties, elemental and
30 mineralogical composition and the carrying out of radiocarbon dating, along with the
31 study of the coastline of the area in question in terms of its morphodynamics and
32 evolution.
33

34 35 2. THE STUDY AREA

36
37 The study area takes in the site of coastal salt mine of the Roman Age located on the
38 coastal strip of the city of Vigo (NW Spain, Figure 1) on the lower slopes of the "Monte
39 Castro" hill which looks over the city. These days, this area is separated from the coast
40 by a relatively flat area produced by land reclamation processes which were carried out
41 during the last third of the 20th century as part of the city's expansion to enable the
42 growth of its commercial port (Castro Carrera, 2007). This part of the city of Vigo
43 corresponds to a relatively shallow inlet modelled on schist rocks, flanked on the SW by
44 the coarse-grained granite projection of Punta De A Laxe and to the NE by the gneisses
45 of Punta da Guía (IGME (the Geological and Mining Institute of Spain), 2012). The old
46 beaches of O Areal and Guixar occupied this inlet, between Punta de A Laxe and Punta
47 de Sta. Tegra, which was located in the Guixar area.
48

49
50 The archaeological remains with which this study is concerned are the "Salt mine of O
51 Areal", which is located in the street of the same name and on the afore-mentioned O
52 Areal beach. They present a series of characteristics which increase their exceptionality
53 among other such sites dedicated to the exploitation of salt of the same age. These types
54 of archaeological structures are not only the largest found in Galicia but are also of the
55 few in such a good state of preservation (Castro Carrera, 2007). Their location on the
56 Atlantic coast is not common for this type of industry, due to the particularities of the
57 climate in the area, with a high rate of precipitation and a lack of strong sun radiation
58
59
60

1
2
3 and the absence of large areas for their installation (Alonso Villalobos & Menanteau,
4 2006). This site, along with another, known as the “Salt mine of Rosalía de Castro”
5 (Martinez Cortizas & Costa Casais, 2008; 2009), formed part of an industrial salting
6 complex during the Roman period. The archaeological structures found at the first of
7 these sites were dedicated to the final process of obtaining salt.
8

9 10 **3. MATERIALS AND METHODS**

11 **3.1 Pedo-sedimentary study**

12
13
14 Five sampling points were selected, from which three were chosen for the purposes of
15 this study, due to their greater variability in terms of facies and thickness. Three
16 sequences were sampled (Ce1, Ce2 and Ce3; Figure 2), which were correlated with the
17 layers of support and filling-in of the salt mine. The structures of the salt mine are
18 located on a small silt pavement on the sands of the beach. Sequence Ce2 formed part of
19 the filling-in of an archaeological structure, possibly associated to a water channel.
20

21
22 The stratigraphy for each of the sequences analysed was defined from the field study
23 (provided by the archaeological company Anta de Moura S.L., who were responsible
24 for carrying out the sampling of the site) and the laboratory work (carried out by our
25 own research group). The taking of samples was carried out from bottom to top,
26 extracting sections with a thickness of between 5 and 1.5 cm, depending on the
27 stratigraphic layer, with the aim of obtaining a better resolution. The samples were air-
28 dried and sieved to separate the thick fraction (> 2mm) from the fine earth fraction (< 2
29 mm). Granulometric and soil reaction (pH) analyses were carried out on the latter in
30 water and KCl. The study of the size of the particles was performed on the ash resulting
31 from burning the samples at 550°C for 5 hours. The mineralogical study, by way of X-
32 ray diffraction with a Philips PW1820, was carried out on selected samples which were
33 associated with the main points of geochemical and stratigraphic change.
34

35
36 The study of the elemental composition was carried out with a LECO Elemental
37 Analyzer, model CNS-2000 for C, N and with an X-ray fluorescence device for Si, Al,
38 Fe, Ti, K, Ca, Zr and Sr. Both of the machines belong to the RIAIDT (Rede de
39 Infraestrutura de Apoio a Investigação e o Desenvolvimento Tecnológico - Network of
40 Infrastructures to Support Research and Technological Development) of the University
41 of Santiago de Compostela.

42
43 In order to establish the morphosedimentary evolution of the site in its chronological
44 context, radiocarbon dating was performed on selected samples. Those located in well-
45 defined stratigraphic layers with abrupt changes in sedimentation and/or in the values of
46 geochemical data were chosen. They were pre-treated, shaking subsamples of the fine
47 earth fraction for 16 hours in ultrapure water. Then, they were filtered through a 50 µm
48 mesh sieve in order to separate sand, roots and other undecomposed organic remains.
49 The resulting suspension was dried in an air heater at a temperature not higher than
50 35°C and then ground. The ¹⁴C measurement via accelerator mass spectrometry (AMS)
51 was carried out in the laboratory of Beta Analytic Inc. (Miami, USA). The results were
52 calibrated using the CALIB 6.0.1 program (Stuiver & Reimer, 1993; Reimer et al.,
53 2009) and were expressed in calibrated years BP (cal BP).
54
55
56
57
58
59
60

3.2 Morphodynamic changes in the coastline of Vigo

The study of the morphodynamics of the coast was carried out on the area of coastline in which the archaeological site is situated. The limits of the ancient coastline were obtained via the georeferencing of 19th century maps dating from before the construction of the port.

A calculation of the flow accumulation was made, with the aim of determining the potential drainage network, using a 25 m Digital Elevation Model (DEM) employing ArcGis 9.3 software.

4. RESULTS

4.1 Pedo-sedimentary study

4.1.1 Stratigraphy and grain size

The three sedimentary sequences were characterised by the fact that they alternate between: (a) layers made up of fine material, brownish sand-silt or silt-sand; (b) silt-clay or clay-silt layers which are grey in colour with bands of iron and (c) layers of coarse-grained or fine sand with either a horizontal or crossed stratification and, in some cases, enriched by iron oxides. A granulometric study complemented and expanded the data obtained in the field. Based on this information, the morphological characteristics of each of the sequences were defined.

CE1

This is the sequence that has the greatest thickness (250 cm). Fifty samples were taken of this sequence (see Figure 3). Two stratigraphic layers can be defined (I and II).

I. Formed by bands of coarse sand (30-90%), with or without Fe precipitates (Ia/Ib, see Figure 3), with horizontal stratification, interspersed with bands of grey silt of lesser coarseness, with an abundance of organic remains (woods) and charcoals. Two sub-layers can be distinguished (Ia and Ib, Figure 3).

II. Characterised by its higher content of silt and clay (40-60%) and the presence of fragmented and eroded archaeological material. At its base (IIa, see Figure 3), the content of fine material and iron oxides is greater, as is the presence of rounded gravel. On the surface (IIc, see Figure 3) it has an abundance of charcoals which are small in size. This sub-layer can be identified archaeologically with the time of its use, following the abandonment and collapse of the salt mine. It would correspond to a necropolis used, according to archaeologists, between the 4th and 7th centuries A.D. (data from the archaeological company “Anta de Moura”).

CE2

This sequence has a thickness of 73.5 cm and 18 samples were taken from it (Figure 4). Six stratigraphic layers were identified, three of them were sandy and three had alternating layers of silt and clay. They presented macro-charcoals.

I, III, V. These were composed of coarse sand with a crossed stratification and a high content of iron oxides in the form of Fe spots or bands of precipitation. They are made up of coarse sand (more than 60% in the case of layers I and III).

II, IV, VI. These were composed of fine compacted silt, with features of oxidation of iron composites. Granulometrically, the fine silt and clay fraction is dominant (>50%),

with sub-layer IV (Figure 4) showing the highest layer of content (up to 75%).

CE3

This sequence has a thickness of 197 cm, with 42 samples being collected (Figure 5). Two stratigraphic layers can be distinguished (I, II, see Figure 5). This is the sequence that presented the greatest content of sand to the detriment of fine material (silt and clay).

I. This is the basal layer. It is made up of sand (mainly coarse) with a horizontal or crossed stratification or banded by iron oxides, forming horizontal lines on the sand.

II. This consists of fine material which is brown-grey in colour, rich in sand and mixed with silt and clay (>40%). It contains a significant amount of fragmented archaeological material. The quantity of silt and clay lessens gradually towards the surface and three sub-layers can be distinguished. IIa, with a thickness of 1.5 cm (see Figure 5), is located 95 cm below the surface. It has the highest content of silt and clay and iron oxide precipitates. The archaeological data indicates that this layer corresponds to the time of use of the salt mine.

4. 1. 2 Soil/sediment reaction (pH)

The reaction of the soil in water is similar in the cases of sequences Ce1 and Ce3, giving values higher than 6.0. In the case of Ce1, it varies from slightly acidic (6.0-7.0) to neutral-alkaline (7.0-8.0), with the highest levels being obtained in the basal layer, coinciding with the high content in coarse sand. The pH values are more homogeneous in the layers which are rich in fine material. The minimum level can be noted at a depth of 200 cm, coinciding with a band of silt (Figure 6). In Ce3, the values are more stable, between neutral-alkaline (between 7.0 and 8.0). The lowest pH values were found in the basal layer, which is rich in coarse sand, whereas its progressive increase coincides with the finer layers.

In Ce2, the reaction of the soil changes in comparison with the previous sequences, with lower values oscillating between extremely acidic (<3.5) in layers II, III and part of layer IV, and acidic-slightly acidic (>3.5-6.5) in layer I and part of IV, V and VI (Figure 6).

The pH in KCl follows extremely similar patterns of variation to those described for the pH in water but with 0.1 to 1.4 units less.

In general, the soil reaction separates the sandy sequences of Ce1 and Ce3, of a neutral-alkaline tendency, from sequence Ce2, which is rich in silt and clay, with a pH ranging from extremely acidic to slightly acidic.

4. 1. 3 The elemental composition of the organic matter

The carbon (C) content of the sequences is generally low: Ce2 (0.05-1%); Ce1 (0.03-1.15%); Ce3 (0.03-0.85%) (Figure 7). The highest values are associated with the layers of fine material (silt-clay). For this reason, sequence Ce2 is the one which shows the highest values, especially in layer IV (up to 2.5%). In sequences Ce1 and Ce3, the carbon content is lower, except in the layers which have bands of silt and clay.

Nitrogen (N) follows a similar pattern of variation to that of carbon: Ce1, 0.04-0.12%; Ce2, 0.05-0.18%; Ce3, 0.04-0.08%. In sequences Ce1 and Ce3, sulphur (S) does not follow a defined pattern, oscillating between values of less than 10 $\mu\text{g g}^{-1}$ and 400 $\mu\text{g g}^{-1}$, reaching maximums in the basal layer of >800 $\mu\text{g g}^{-1}$ and 0-300 $\mu\text{g g}^{-1}$ respectively. In Ce2, the values are higher, with concentrations oscillating between 200 $\mu\text{g g}^{-1}$ and

21.000 $\mu\text{g g}^{-1}$, with maximums between layers II and IV (see Figure 7), coinciding with the lowest pH values.

4. 1. 4 *The elemental composition of the mineral fraction: Si, Al, Fe, Ti, K, Ca, Zr and Sr*

The description of the characteristic chemical elements of the inorganic or mineral fraction, majority or minority elements (Si, Al, Fe, Ti, K, Ca) and part of the lithogenic trace elements (Zr, Sr) is included in this group, due to the fact that they are conservative elements.

The elements analysed in the three sequences show similar ranges (Figure 8). Al, Fe, Ti, and Zr present a similar pattern of variation: lower concentration and higher variation in the sandy layers and maximums in the silt-clay layers or in the layers enriched with iron oxides. These elements present a positive correlation with the silt-clay fraction, $r=0.87$, 0.92 , 0.90 and 0.82 respectively. However, Si, K and Sr follow an inverse pattern to the previous elements, which is correlated with the coarse sand fraction (Si $r=0.87$, K $r=0.69$ and Sr $r=0.63$). Calcium and Sr are negatively correlated in Ce1 and Ce3 ($r=0.71$ and $r=0.78$ respectively), whereas in Ce2 no correlation can be observed. Zirconium presents a higher level of concentration in the layers which are rich in silt and clay.

Sequences Ce1 and Ce3 present a similar evolution. They are formed by a basal layer, which is rich in coarse sand, Si, K and Sr, and a superficial layer with a higher content of silt, clay, Al, Fe, Ti, Ca and Zr. At the base of Ce1 accumulations of silt and clay and interspersed precipitates of iron oxides can be noted. In Ce3, the superficial samples presented similar granulometric and compositional characteristics to the basal layers (Figure 8).

Sequence Ce2 alternates more between sandy layers with precipitates of iron oxides and silt and clay, which is reflected in its elemental composition. The sandy layers (I, III and V, see Figure 8), are rich in Si, K and Sr, whereas the silt-clay layers (II, IV and VI) are rich in Al, Fe, Ti and Zr. Calcium does not present significant variations in depth.

4. 1. 5 *Mineralogical composition*

The samples analysed in the three sequences contain: quartz, feldspar, mica, interstratified mica-vermiculite, 1:1 dioctahedral phyllosilicates of a kaolinite gibbsite type (Table II).

Quartz and 1:1 dioctahedral phyllosilicates are the most abundant minerals and their distribution follows an inverse pattern (Table II). In turn, the samples which are rich in quartz contain more than 50% sand and those rich in 1:1 dioctahedral phyllosilicates contain more than 40% silt and clay. This indicates that mineralogy is determined by the granulometrics of the sediment.

The relative abundance of feldspars and micas is less (between present and trace). The mica is of a muscovite type and its abundance is greater in the samples which are richer in 1:1 dioctahedral phyllosilicates. Within the feldspars, potassium feldspar (microcline) and plagioclase can be identified. In general, the sandy samples, with a higher quartz content, also present a higher concentration of feldspars, with greater or the same abundance relative to the two types described, whereas in the samples with a higher concentration of 1:1 dioctahedral phyllosilicates, plagioclases are more abundant than microcline. Gibbsite and interstratified mica-vermiculite appear as traces and follow a similar

4.2 Morphodynamic changes in the coastline of Vigo in Roman times

The scarcity of available paleo-environmental and archaeological information does not permit the position and configuration of the coastline in Roman times to be established with any great precision. However, it is possible to consult documentation from 19th century maps plotted prior to the construction of the different phases of the port of Vigo, assuming that the configuration of the sedimentary bodies reflected therein responds to natural morphodynamic parameters. In these maps, the beach of O Areal constitutes a continuous sedimentary complex, with a broad intertidal surface and an extremely dissipative profile, extending towards the east (Figure 9). Opposite the rocky outcrop of Punta de A Laxe, where a bulwark was situated, a much narrower beach must have existed, probably of coarser sediment which would have been completely submerged at high tide.

Towards the north-east, the topography becomes more abrupt and, approximately from the modern-day street named Isaac Peral, the lay of the land suggests the existence of a stretch of cliff, which limited the internal part of the beach (Figure 10).

The coastline is an approximate reconstruction of the position of high tide prior to the construction of the port at the beginning of the 20th century.

Today, the wave regime corresponds to a low energy coast, as is expected for an internal sector of a Ria, protected by the Cies Islands. There is no wave data available for the Ria. However, we used the data from a point of the model of wave propagation of the Spanish Port Authority (point WANA-1044069, situated to the west of the Cies Islands indicates that 80% of the waves are between 1 and 3 metres in significant height, principally in the fourth (80%) and third (11%) quadrants (Puertos del Estado, 2012). However, the location of the Port of Vigo, in an internal sector of the ria, means that waves from open waters can only spread in a highly attenuated manner and from the west or west-north-west, which should result in a drift towards the east, partly nourished by the sediment coming from the ancient beaches of Bouzas, Coia and San Francisco. This was the documented cause of the silting of the iron dock built in Punta de A Laxe at the end of the 19th century (Garrido Rodríguez, 2001).

The majority of the urban centre of Vigo is shaped in the form of an amphitheatre, in which the drainage surface is necessarily reduced. In an attempt to reconstruct the main flow lines, the potential drainage network was extracted from 5 and 25 m Digital Elevation Models (DEM) from Spanish National Geographic Institute. Even taking into account the fact that both are cases of DEMs in which the configuration of the land reflects modifications produced by the urban development of the city, the eastern sector of the beach can easily be identified as having a drainage network with greater flow accumulation (Figure 11).

5. RESULTS AND DISCUSSION

5.1 The evolution of sequences Ce1, Ce2 and Ce3

These sequences are characterised by the fact that they present alternate sandy and silt-clay layers, which are associated with a specific soil reaction and a specific elemental and mineralogical composition.

The coastal system: beach facies

This sedimentary formation is identified in the sandy layers of sequences Ce1 (layer Ia,b) and Ce3 (I and IIc) (see Figure 12). It presents slightly acidic to neutral-alkaline pH values (5.0-8.0), a higher content of coarse sands, Si, K and Sr, quartz and potassium feldspar (microcline). It mainly consists of coarse sands which are rich in quartz and potassium feldspar, resistant minerals which are concentrated in the coarser fractions as resistates. Potassium feldspar is a mineral which does not alter much, therefore it commonly appears with sandy fractions, be they coarse or fine. Sr is associated with sands due to the fact that it is a mineral with a coarse fraction. Its presence is determined by the isomorphic substitution of the Ca, which indicates possible inclusions of calco-sodic feldspars. These layers also present crossed or horizontal stratification, with a high level of Fe content and, in some cases, they are interspersed with fine material. Furthermore, in the field, flat rounded gravel was observed, along with marine erosion in the sands (Barral, Guitián, & Guitián Ojea, 1985; Costa, Martínez & Pérez, 1994; Martínez et al, 1997). Its situation in a coastal sector and the morphometric characteristics present in the sands indicate a marine origin.

The system of continental and marine interaction: "lagoon" facies

This sedimentary formation can be identified in the silt-clay and silt-sand layers of sequences Ce1 (II a, b, c) and Ce3 (II a, b). It contains a higher degree of content in silts, clays, Al, Fe, Ti, Ca, Zr, C, N, 1:1 dioctahedral phyllosilicates, plagioclases and traces of gibbsite and interstratified mica-vermiculite. Its pH values range from slightly acidic to neutral-alkaline (5.0-8.0). Its origin can be related to the development of low energy fresh water courses which may have formed small channels where water would have flowed slowly, thus favouring the decantation of fine material, which would progressively block these channels. The type of sediment deposited is essentially of continental origin, coming from mineral weathering and the precipitation of secondary compounds. The result of this is that they are dominated by fine minerals which are rich in Al, Fe and Ti, such as 1:1 phyllosilicates of a kaolinite type, interstratified mica-vermiculite, gibbsite and minerals rich in Ca, such as plagioclases, with a high degree of alterability. They also present zircons and are enriched in organic material (a higher C and N content), due to its fine nature.

The anthropized intertidal System: "marshland" facies

This sedimentary formation can be identified in sequence Ce2, in the silt-clay layers II and IV and in the sandy layer III. Its elemental and mineralogical composition is very similar to that of the sandy and silt-clay layers described previously, albeit with a high content of organic material, low pH values (<3.0, extremely acidic) and a high degree of S. These are typical characteristics of acid sulphate soils formed in coastal marshland, preferably on fine sediment which is rich in sulphurs which, due to oxidation, generate a high degree of acidity (Schlesinger, 2000; Otero & Macías, 2001). According to the

1
2
3
4
5
6
7
8
9
10
11
12
13
14
15
16
17
18
19
20
21
22
23
24
25
26
27
28
29
30
31
32
33
34
35
36
37
38
39
40
41
42
43
44
45
46
47
48
49
50
51
52
53
54
55
56
57
58
59
60

FAO-WRB (2006), these acid sulphate layers can be classified as hyperthionic fluvisols due to their low pH values. Their formation depends on sediments which are rich in fine material (fine sands and/or silt and clay) being flooded by sea water (rich in sulphates), thus favouring the precipitation of sulphurs in these layers. The variations in redox conditions, due to the fact that they are developed in an intertidal zone, lead them to become acidified by the oxidation of the sulphurs and cause them to evolve towards soils of an acid sulphate type. The high degree of content of organic material is associated with *in situ accumulation* by biological colonization typical of coastal marshland areas and by the deposition of fine material which is trapped in the vegetation network. They are formed in the area behind the beach, in water channels or small intertidal areas with a certain degree of biological colonization, in which marshland would develop. The sedimentary formations of this type are characterized by acid sulphate layers which are rich in organic material, marine sands and fine material of continental origin. Layers with these characteristics can be identified exclusively in layers II, III and IV of sequence Ce2 (see Figure 12), although the remaining layers of this sequence are also related with similar dynamics but cannot be classified as acid sulphate soils, possibly due to the fact that they received less influence from the sea. Archaeological information on this sequence suggests it is related with the filling in of a water-channelling structure for the salt mine. For this reason, its physical and chemical characteristics are linked to anthropic processes as well as to natural ones.

Figure 12 shows a stratigraphic synthesis of each of the sequences. Sequences Ce1 and Ce3 have similar patterns with a basal layer of the beach which is truncated by a layer of silt and clay. The discontinuity between them indicates an abrupt change in sedimentation, from one of a coastal environment, controlled by marine process, to one of continental-marine interaction, dominated by the sedimentation of fine material which is essentially of continental origin. Although they follow an almost identical pattern, they have differences as far as granulometry and mineralogy are concerned, with sequence Ce3 being sandier and richer in quartz. Ce2 presents a greater alternation between sandy and silt-clay layers, whose physical and chemical and sedimentological properties are related with an intertidal system of a marshland type, which was possibly modified by the use of the salt mine.

5. 2 Chronostratigraphic reconstruction

The sector in question, which is currently situated in the centre of the city of Vigo (in the province of Pontevedra), is a sedimentary fossil environment which is highly complex and characterized by its anthropic use both in space and time, in which structures connected to human activity are mixed with those of a natural sedimentary origin.

Radiocarbon dating of the oldest layers corresponds to the base of sequences Ce1 and Ce3, with beach deposits which would have been formed under marine influences and would have originated before 1540-1420 BC and 1980-1760 BC respectively (Table I, Fig. 13). From 1500 BC onwards, these dynamics were truncated and sedimentation of fine material of continental origin began. This process continued until 790-450 BC, at least in the area in which sequence Ce 1 is located. In this sequence and in Ce3 the sedimentation has a “lagoon” facies while sequence three has a “marshland” facies. The pedo-sedimentary interpretation of these sequences suggests a progressive continentalisation of morphogenetic processes. The sedimentation of fine material of continental origin over the beach layers would imply the evolution of the environment

1
2
3 from a marine system to a system of greater marine-continental interaction.

4 Radiocarbon dating proves a chronological continuity in the sequences, with the
5 exception of the upper part of Ce1, in which there is a temporal hiatus from 790-450 BC
6 to 220-400 AD. The superficial layer of this sequence correlates chronologically with a
7 necropolis dated archaeologically between the 4th and 7th centuries AD. In turn, part of
8 this hiatus would coincide with the Roman Period (see Figure 13) and, therefore, could
9 be associated with the exploitation of the salt mine.

10
11 The initial chronostratigraphic proposal for this sector, based on archaeological data
12 (ceramic remains), interpreted the sediments rich in fine material of sequences Ce1 and
13 Ce3 as continental filling, dated later than the use of the salt mine and attributed them to
14 the late Roman Period. In addition, the exploitation of the salt mine was placed in the
15 first silt layers of both sequences, situated on the sands of the beach (see Figure 13). In
16 this way, sequences Ce1 and Ce3 would be contemporaneous and the formation of the
17 layers of silt would be related with anthropic use.

18
19 The archaeological hypothesis contemplated that the base of the silt layers of Ce1 and
20 Ce3 could correspond to the layer of the use of the salt mine. However, the age given by
21 radiocarbon dating (1300-1020 BC and 1540-1420 BC respectively) situates them long
22 before the Roman Age. Only the upper part of sequence Ce1 correlates with the Roman-
23 late Roman Period and the exploitation of the salt mine. The differing thickness of the
24 silt-clay layer of the three sequences analysed may reflect their conditioning prior to the
25 exploitation being carried out, in order to obtain an appropriate level to allow for the
26 suitable circulation of water in the salt mine, which would have caused part of the
27 truncation of the previous deposits and the absence of the most recent layers.

30 **5. 3 The Reconstruction of the Coastline of the “O Areal” sector**

31
32 Reconstructions of the rising of the sea level in the Late Holocene in the north west of
33 the Peninsula indicate a eustatic maximum which probably occurred between 5000 and
34 2500 BP, following which a relative fall and a new rise occurred until the sea level
35 stabilized at its current level not before 3000 years BP (Bao et al., 2007; Dias et al.,
36 2000; Costas-Otero et al, 2009). The pedo-sedimentary record studied in the Rosalía de
37 Castro and O Areal sites (Tallón Armada, 2012; Tallón Armada et al, 2013) appears to
38 point towards this theory, with a stabilization of the sedimentary system after 3500 BP
39 with the formation of the fluvial-marine complex. However, some authors have
40 suggested the existence of a transgressive pulsation with a higher sea level than today
41 around 2000 yr BP (Granja et al, 1996; Martinez Cortizas & Costa-Casais, 1997). The
42 elevation at which the pavement of the salt mine is situated shows a considerable
43 variation in the sites, between 2.6 and 3.7 m above geodesic zero. The current mean
44 tidal range is 2.4 m, with a maximum astronomic spring range of 4.19 m. The maximum
45 atmospheric surge registered between 1993 and 2003 is 0.69 m, although return periods
46 of more than 300 years have been calculated for surges of more than 0.9 m (Puertos del
47 Estado, 2005). If the elevations refer to the lowest low tide, we find that the pavement
48 of the salt mine lies between the tidal elevations of 4.4 and 5.5 m, in other words, higher
49 than the elevation of the maximum astronomic tide registered in Vigo’s tidal gauge.
50 This fact appears to suggest that the sea level was higher than it is today during the
51 period of exploitation of the salt mine, although it is necessary to be extremely prudent
52 in this regard given the number of factors which could affect the elevations referred to
53 here, from morphodynamic aspects of the beach itself to aspects concerning the working
54 of the salt mine.

55
56 The pedo-sedimentary record studied in the Rosalía de Castro and O Areal sectors
57
58
59
60

(Tallón Armada, 2012; Tallón Armada et al, 2013) suggests a process of stabilisation and progradation of the coastline following the stabilisation of the sea level around 3500 BP. When the Holocene sea-level rise stopped, the coastal system began a stage of reorganization, leading to the configuration of a beach-dune complex, which gave rise to the formation of a fluvial-marine system. Later, the whole coastal system underwent changes in its configuration, possibly as a response to forcing of a climatic or morphodynamic nature, essentially characterised by oscillations in the aeolian activity and the position of the dune system, as well as by variations in the inputs of sediments of continental origin. Furthermore, given that the sedimentary sequence corresponds to a record on a highly modified environment, human activity significantly affected the evolution of the system during and after the period of the exploitation of the salt mine.

6. FINAL REMARKS

The evolution of the study area was conditioned by its coastal position and its relationship with the city of Vigo. The main changes observed in the pre-Roman Age are associated with the evolution of climate during the late Holocene, which led to progradation, stabilization and the reconfiguration of the coastline, which would go on until the Roman Age. This is reflected in the pedo-sedimentary characteristics of the sequences from O Areal analysed and described in this paper and in those of the adjacent archaeological site of Rosalía de Castro described in Tallón Armada (2012) and Tallón Armada et al. (2013). The salt mining, which occurred in this place, provides evidence of certain conditions concerning climate, morphogenetics and land occupation. The evolution of the coastal system from beach to marshland offered the appropriate conditions for the installation of a salt mine. This activity probably developed due to more favourable climatic conditions (the Roman Warm Period had less precipitation and more solar radiation; Martínez Cortizas & Vázquez Varela, 2002) and a possible transgressive pulse or final reconfiguration of the coastline associated to the rising sea level of the Holocene. Furthermore, as the remains found between the sector of O Areal and Rosalía de Castro bear witness, the extension of the occupation, as is proper for an industrial activity (Curras, 2007), would have taken in an extremely broad strip of the coastline. This demonstrates the importance of the exploitation of salt in the Roman Age and also the relevance of the city of Vigo as far as this essential industry of the Roman Empire is concerned. Between the 4th and 7th centuries AD, the site became abandoned, which led to the consequent spatial reconfiguration of the area and its later use as a necropolis (Memoria técnica de excavación -Technical excavation report, 2007).

Urban growth and new spatial dynamics led to a change in the position of the site with regard to its city of reference. It went from occupying an outlying position of an industrial kind to becoming incorporated within the city by fossilization. However, this circumstance changed when the remains were exhumed. At this point geoarchaeological research intervened, providing essential information about the environmental and archaeological context of the site for its enhancement. From this moment on, the archaeological remains took on a new meaning for the city due to the information provided about its past. Thus, they became integrated into the city with a new focus via the dissemination of the idea that Vigo had an important settlement based on the exploitation of salt and, on the basis of this industrial activity, the city was an integral part of the commercial networks of the Roman Age, which, without doubt, contributes towards forming a new vision of the current city of Vigo.

The fact of converting this site into a museum increases its value for the city, making it part of its cultural heritage. At the same time, the associated pedo-sedimentary deposits

1
2
3 should also be considered as part of this (geological) heritage in that they are records
4 that provide essential information regarding the environment and human activity, which
5 enables us to understand and recognize the past. Therefore, in archaeological
6 excavations in urban areas, geoarchaeological work should be considered essential as
7 far as the historical interpretation of the city in question is concerned.
8

10 ACKNOWLEDGMENTS

11 This work has been partially developed in projects “Realización de análises
12 paleoambientais e arqueométricas do Xacemento do Areal” (Dirección Xeral de
13 Patrimonio, Consellería de Cultura e Deporte), “Xeoarqueoloxía reconstrución
14 paleoambiental. Metodoloxía aplicada a contextos arqueolóxicoculturais”
15 (90SECO15606PR, Consellería de Economía e Industria), GPC2014/009 and R2014-
16 0001 (Rede Consiliencia) funded by Xunta de Galicia. We thank Juan Carlos Castro
17 (Anta de Moura) for his help with the archaeological information and the
18 documentation provided to us.
19
20

22 REFERENCES

23
24 Alonso Villalobos, C., & Menanteau, L. (2006). Paleóenviroments e techniques de
25 production du sel marin (par ignition ou insolation) durant l'Antiquité: les cas des baies
26 de Bourgneuf (France) et de Cadix (Espagne). In J.C. Hocquet, J.L. Sarrazin, G. Buron
27 (Coords.). *Le Sel de la Baie. Histoire, archéologie, ethnologie des sels atlantiques*,
28 *Histoire*, 87-103. Presses Universitaires de Rennes.
29

30
31 Bao, R., Alonso, A., Delgado, C., Pages, J.L. (2007). Identification of the main driving
32 mechanisms in the evolution of a small coastal wetland (Traba, Galicia, NW Spain)
33 since its origin 5700 cal yr BP. *Palaeogeography, Palaeoclimatology, Palaeoecology*
34 247, pp. 296– 312
35

36
37 Barral Silva, M. T., Guitián Rivera, F., Guitián Ojea, F. (1985). Estudio
38 sedimentológico de un depósito arenoso de la rasa Cantábrica. Aplicación de la
39 exoscopia del cuarzo. *Cuadernos do Laboratorio Xeolóxico de Laxe*, 9, 329-347.
40

41
42 Bini, M., Chelli, A., Maria, A., Gervasini, L., Pappalardo, M., (2007).
43 Geoarchaeological sea-level proxies from a silted up harbour : A case study of the
44 Roman colony of Luni (northern Tyrrhenian Sea , Italy). *Quaternary International*, 206,
45 1-2, 147-157.
46

47 Butzer, W. K. (1982). *Archaeology as human ecology*. Cambridge: University press.
48

49 Butzer, K. W. (2008). *Geomorphology Challenges for a cross-disciplinary*
50 *geoarchaeology : The intersection between environmental history and geomorphology*,
51 101, 402-411.
52

53
54 Butzer, W. K., Butzer, E., Love, S. (2013). Urban geoarchaeology and environmental
55 history at the Lost City of the Pyramids, Giza: synthesis and review. *Journal of*
56 *Archaeological Science*, 40, 8, 3340–3366.
57
58
59
60

1
2
3 Benedetti, M.M., Cordova, C.E., Beach, T. (2011). Soils, sediments, and
4 geoarchaeology: Introduction. *Catena*, 85, 83–86.

5
6 Cinti, M., & Huisman, J. D. (2015). Scientific advances in geoarchaeology during the
7 last twenty years. *Journal of Archaeological Science*, 56, 96–108

8
9 Castro Carrera, J. C. (2007). La salina romana del yacimiento de “O Areal” Vigo,
10 (Galicia): un complejo industrial salazonero altoimperial. In L. Langóstena, D. Bernal,
11 A. Arévalo (Eds.). *Salsas y salazones de pescado en Occidente durante la Antigüedad*,
12 *Actas del Congreso Internacional CETARIAE*, 355-365. *British Archaeological*
13 *Reports*, International Series 1686.

14
15
16 Costa Casais, M., Martínez Cortizas, A., Pérez Alberti, A. (1994): Caracterización de un
17 depósito costero de la Ría de Muros-Noia (La Coruña, Galicia). En J. Arnaez, J. M.
18 García Ruíz & A. Gómez Villar (Eds.): *Geomorfología en España*, tomo I, *Sociedad*
19 *Española de Gemorfología*, Logroño. 355-368.

20
21
22 Costas-Otero, S., Muñoz Sobrino, C. Alejo, I., Pérez-Arlucea, M. (2009). Holocene
23 evolution of a rockbounded barrier lagoon system, Cíes Islands, northwest Iberia. *Earth*
24 *Surface processes and Landforms* 34, pp. 1575-1586

25
26 Currás, B. (2007) .Aportación al conocimiento de la industria de salazon en las Rias
27 Baixas gallegas In L. Langóstena, D. Bernal, A. Arévalo (Eds.). *Salsas y salazones de*
28 *pescado en Occidente durante la Antigüedad*, *Actas del Congreso Internacional*
29 *CETARIAE*, 135–149. *British Archaeological Reports*, International Series 1686.

30
31
32 Dias Alveirinho, J.M.A., Boski, T., Rodrigues, A., Magalhães, F. (2000). Coast line
33 evolution in Portugal since the Last Glacial Maximum until present –a synthesis.
34 *Marine Geology* 170 (1-2), pp. 177-186

35
36 Dincauze, D.F. (2000). *Environmental archaeology: principles and practice*. Cambridge:
37 *University Press*.

38
39
40 FAO. (2006). A framework for international classification, correlation and
41 communication. World reference base for soil resources. Food and Agriculture
42 organization of the United Nations, Rome.

43
44 Garrido Rodríguez, J. (2001). *El puerto de Vigo. Síntesis histórica*. Autoridad Portuaria.
45 *Consortio de la Zona Franca de Vigo*. 359 pp.

46
47 Granja H.M., & de Groot, T.A.M. (1996). Sea level rise and neotectonism in a
48 Holocene coastal environment at Cortegaça Beach (NW Portugal) – a case study,
49 *Journal of Coastal Research* 12, pp. 160–170

50
51
52 GEODE (2012). *Mapa Geológico Digital continuo de España*. SIGECO. IGME. Editor:
53 J. Navas. Disponible en: <http://cuarzo.igme.es/sigeco/default.htm>

54
55
56 Martínez Cortizas, A., & Costa Casais, M. (1997). Indicios de variaciones del nivel del
57 mar en la ría de Vigo durante los últimos 3000 años. *Gallaecia* 7. 121-135.

1
2
3 Martínez Cortizas, A., & Costa Casais, M. (Cords.) (2008). Estudio estratigráfico e
4 geoquímico do xacemento Unidade II Parcela P3-6 da Rúa Rosalía de Castro (Vigo,
5 Pontevedra). Informe Técnico.
6

7 Martínez Cortizas, A., & Costa Casais, M. (Cords.) (2009). Informe sobre las salinas de
8 época romana (Edificio Sergas, Vigo) Informe Técnico.
9

10 Martínez Cortizas, A., Otero Pérez, X. L., Costa Casais, M. (1996). Edafogénesis
11 cuaternaria del depósito dunar de Figueras (Islas Cíes-NW España): implicacions
12 paleoambientales. Nova Acta Científica Compostelana (Biología) 7, 121-135
13

14 Martínez Cortizas, A., & Vázquez Varela, J.M. (2002). El clima en la Galicia romana:
15 una aproximación interdisciplinar. vista Real Academia Galega das Ciencias, XXI, 87–
16 104.
17

18 Memoria de excavación. (2007). Fase II. Evaluación Patrimonial de la Unidad de
19 actuación I-06. Rosalía de Castro II, Vigo (Pontevedra). Año 2007. Clave: CD 102^a
20 2006/368-0
21

22 Nicoll, K., & Murphy, R.L. (2014): Soil and sediment archives of ancient landscapes,
23 paleoenvironments, and archaeological site formation processes. Quaternary
24 International, 342, 1-4.
25

26 Otero. X.L., & Macías, F. (2001): Caracterización y clasificación de los suelos de
27 marismas de la Ría de Ortigueira en relación con su posición fisográfica y vegetación
28 (Galicia-NO de la península ibérica). Edafología 8, 3, 37-61.
29

30 Panin, A. V., & Bronnikova, M.A. (2014): Human dimensions of palaeoenvironmental
31 change: Geomorphic processes and geoarchaeology. Quaternary International, 324, 1-
32 5.
33

34 Puertos del Estado (2005). Red de mareógrafos de puertos (REDMAR).
35 www.puertos.es.
36

37 Puertos del Estado (2012). Clima medio de oleaje. Nodo WANA1044069.
38 www.puertos.es.
39

40 Quirós, J. A., Nicosi, C., Polo Díaz, A., Ruíz del Árbol, M. (2014). Agrarian
41 archaeology in northern Iberia: Geoarchaeology and early medieval land use.
42 Quaternary International, 346, 26-58.
43

44 Reimer, P. J., Bailie, M. G. L., Bard, E., Bayliss, A., Beck, J. W., Blacwell, P. G.,
45 Bronk Ramsey, C., Buck, C. E., Butt, G. S., Edwards, R. L., Friederich, M., Grootes, P.
46 M., Guilderson, T. P., Hajdas, I., Heaton, T. J., Hogg, A. G., Hughen, K.A., Kaiser, K.
47 F., Kromer, B., McCormac, F. G., Manning, S. W., Reimer, R. W., Richards, D. A.,
48 Southon, J. R., Talamo, S., Turney, C. S. M., van der Plicht, J., Weyhenmeyer, C. E.
49 (2009). IntCal09 and Marine09 radiocarbon age calibration curves, 0-50,000 years cal
50 BP. Radiocarbon 51, 1111-1150.
51
52
53
54
55
56
57
58
59
60

1
2
3 Rothschild, N. A., & Di Zerega Wall, D. (2008). Urban Archaeology. *Encyclopedia of*
4 *Archaeology*, 2164–2171.

5
6
7 Shahack-Gross, R., Albert, R.M., Gilboa, A., Nagar-Hilman, O., Sharon, I., Weiner,
8 S.(2005). Geoarchaeology in an urban context: the use of space in a Phoenician
9 monumental building at Tel Dor (Israel). *Journal of Archaeological Science* 32, 1417–
10 1431.

11
12 Simonson, Schlesinger, W. H. (2000) *Biogeoquímica, un análisis global (1ª edición)*.
13 Barcelona: Editorial Ariel.

14
15
16 Shuldenrein, J., & Aiuvalasit, M. (2011). Urban geoarchaeology and sustainability: a
17 case study from Manhattan Island, New York City, USA. In: A. G. Brown, L. S. Basell,
18 K.W. Butzer (Eds.). *Geoarchaeology, Climate Change, and Sustainability, Special*
19 *Paper*, 476, Geological Society of America.

20
21 Stuiver, M., & Reimer, P. (1993). Extended 14C database and revised CALIB
22 radiocarbon calibration program. *Radiocarbon* 35, 215-230.

23
24 Tallón Armada, R. (2012). Marco evolutivo dunha explotación salineira de época
25 romana (Vigo, Pontevedra). Memoria de Licenciatura. Universidade de Santiago de
26 Compostela.

27
28 Tallón Armada, R., Costa-Casais, M., Taboada, T., Martínez Cortizas, A. (2013):
29 Reconfiguración de la línea de costa en un sector de explotación salinera de época
30 romana en el NO de España. In G. Flor Rodríguez, G. Flor-Blanco, L.A. Pando
31 Gonzalez, (Eds.): *Geotemas: VII Jornadas de Geomorfología Litoral*, Sociedad
32 Geológica de España.

33 34 35 36 **FIGURE CAPTIONS**

37
38 Figure 1. The location of the study area. Maps taken from Google Earth and
39 geographical information from the Xunta de Galicia.

40
41 Figure 2. The location of the archaeological structures and the sites selected for
42 sampling (circles); the studied sequences are labelled (Ce1, Ce2 and Ce3). Map
43 provided by the archaeological company “Anta de Moura”.

44
45 Figure 3. Stratigraphy and grain size distribution of sequence Ce1. (%Cs: percentage of
46 coarse sand; %FS: percentage of fine sand; %S+C: percentage of silt and clay)

47
48 Figure 4. Stratigraphy and grain size distribution of sequence Ce2. (%Cs: percentage of
49 coarse sand; %FS: percentage of fine sand; %S+C: percentage of silt and clay)

50
51 Figure 5. Stratigraphy and grain size distribution of sequence Ce3. (%Cs: percentage of
52 coarse sand; %FS: percentage of fine sand; %S+C: percentage of silt and clay)

53
54 Figure 6. Soil reaction in sequences Ce1, Ce2 and Ce3. pH in KCl, black circles; pH in
55 water, white circles.

56
57 Figure 7. C (%), N (%) and S ($\mu\text{g g}^{-1}$) contents in sequences Ce1, Ce2 and Ce3

58
59 Figure 8. Content of Si (%), Al (%), Fe (%), Ti (%), K (%), Ca (%), Sr ($\mu\text{g g}^{-1}$) and Zr
60

1
2
3 (µg g⁻¹) in Ce1, Ce2 and Ce3.

4 Figure 9. A reconstruction of shorelines from maps produced in 1880 and 1850 AD.

5
6 Figure 10. Topography of the Vigo area taken from the IGN's (Spanish National
7 Geographic Institute) 25 m DEM.

8
9 Figure 11. The potential drainage network calculated from a 25 m DEM.

10
11 Figure 12. A stratigraphic synthesis of the pedo-sedimentary and archaeological features
12 of Ce1, Ce2 and Ce3.

13
14 Figure 13. Chronostratigraphic reconstruction of the sequences studied

15 16 **TABLE CAPTIONS**

17
18 Table I. Radiocarbon dating of selected samples of sequences Ce1, Ce2 and Ce3.

19
20 Table II. Mineralogy of selected samples of sequences Ce1, Ce2 and Ce3. Q=quarz; F:
21 feldspars; M-V: interstratified mica-vermiculite; 1:1: 1:1 dioctahedral phyllosilicates:
22 Gib: gibbsite.
23
24
25
26
27
28
29
30
31
32
33
34
35
36
37
38
39
40
41
42
43
44
45
46
47
48
49
50
51
52
53
54
55
56
57
58
59
60

1
2
3
4
5
6
7
8
9
10
11
12
13
14
15
16
17
18
19
20
21
22
23
24
25
26
27
28
29
30
31
32
33
34
35
36
37
38
39
40
41
42
43
44
45
46
47
48
49
50
51
52
53
54
55
56
57
58
59
60



Figure 1. The location of the study area. Maps taken from Google Earth and geographical information from the Xunta de Galicia.
275x118mm (96 x 96 DPI)

Peer Review

1
2
3
4
5
6
7
8
9
10
11
12
13
14
15
16
17
18
19
20
21
22
23
24
25
26
27
28
29
30
31
32
33
34
35
36
37
38
39
40
41
42
43
44
45
46
47
48
49
50
51
52
53
54
55
56
57
58
59
60

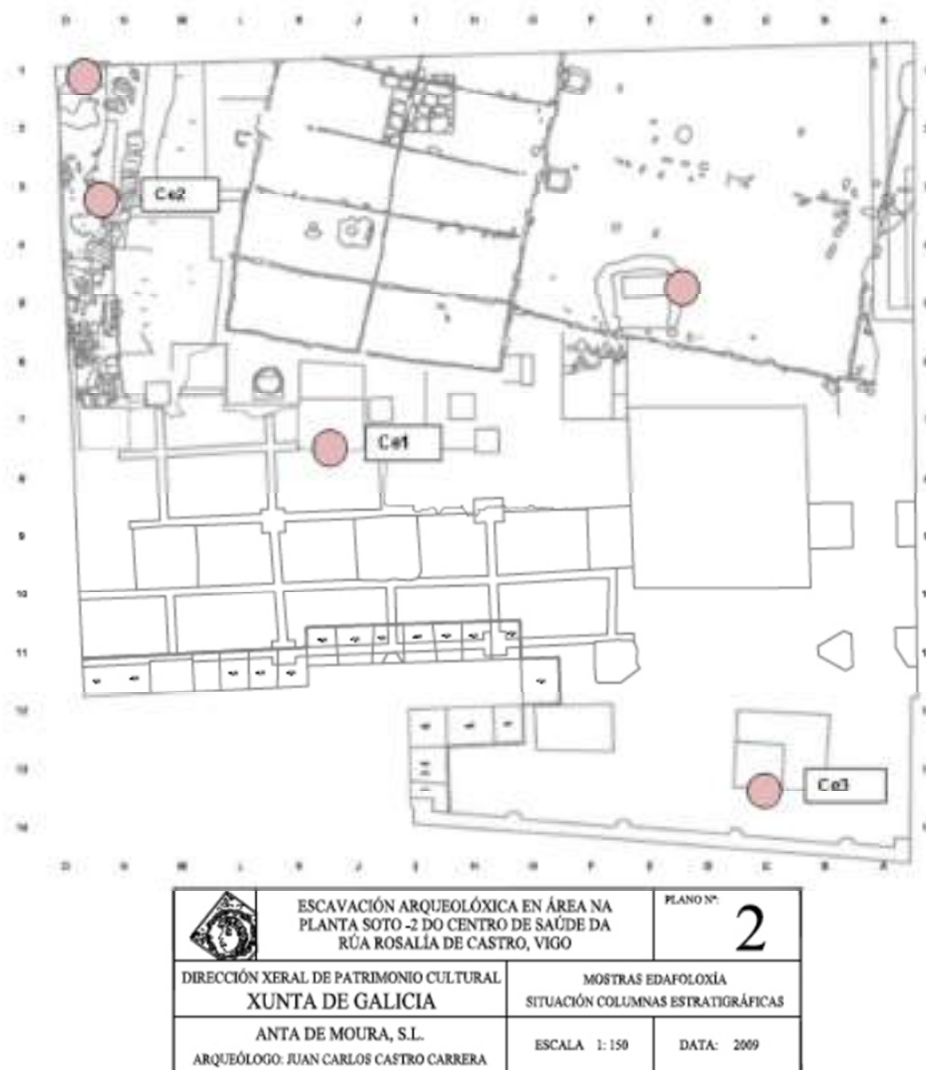


Figure 2. The location of the archaeological structures and the sites selected for sampling (circles); the studied sequences are labelled (Ce1, Ce2 and Ce3). Map provided by the archaeological company "Anta de Moura".
185x202mm (96 x 96 DPI)

1
2
3
4
5
6
7
8
9
10
11
12
13
14
15
16
17
18
19
20
21
22
23
24
25
26
27
28
29
30
31
32
33
34
35
36
37
38
39
40
41
42
43
44
45
46
47
48
49
50
51
52
53
54
55
56
57
58
59
60

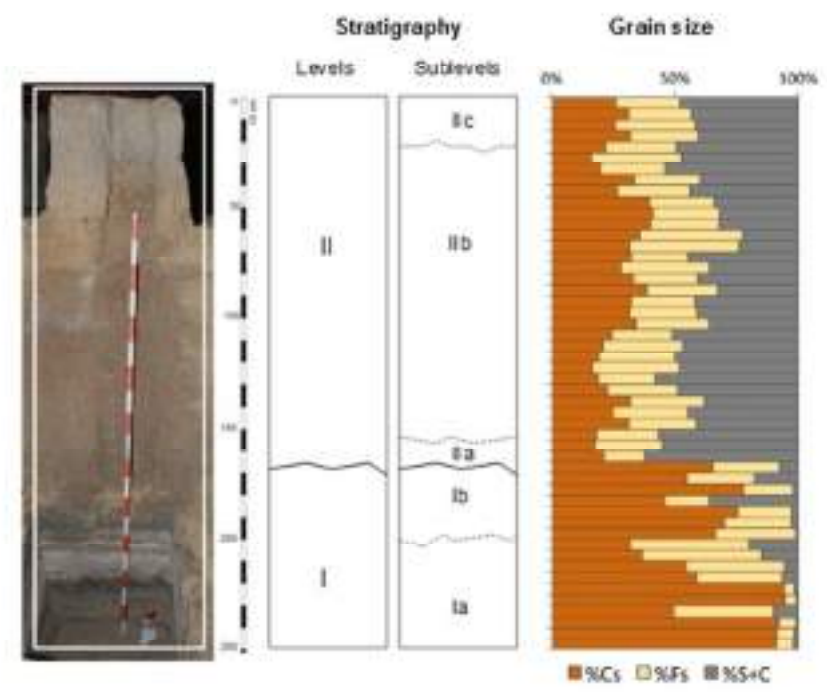


Figure 3. Stratigraphy and grain size distribution of sequence Ce1. (%Cs: percentage of coarse sand; %FS: percentage of fine sand; %S+C: percentage of silt and clay)
161x123mm (96 x 96 DPI)

Review

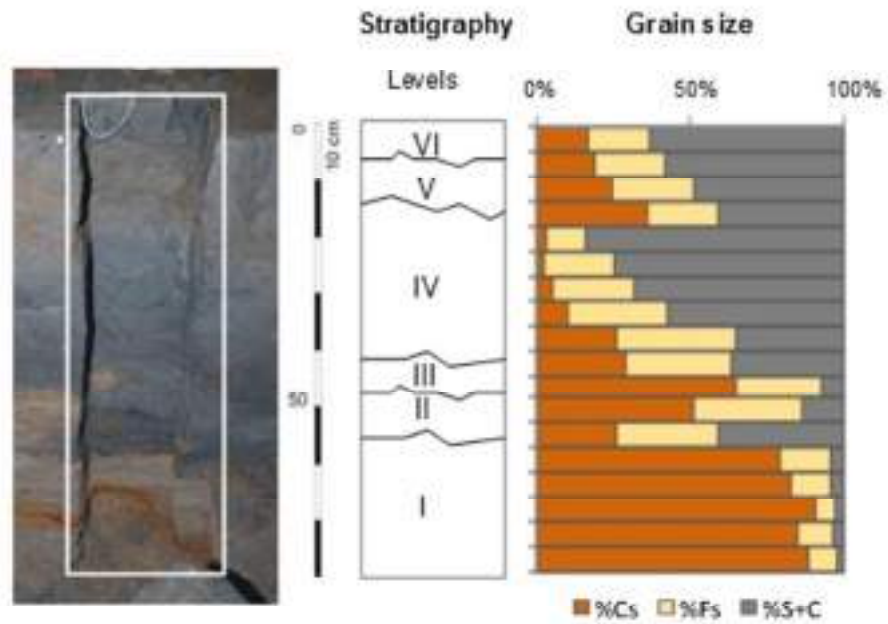


Figure 4. Stratigraphy and grain size distribution of sequence Ce2. (%Cs: percentage of coarse sand; %FS: percentage of fine sand; %S+C: percentage of silt and clay)
127x98mm (96 x 96 DPI)

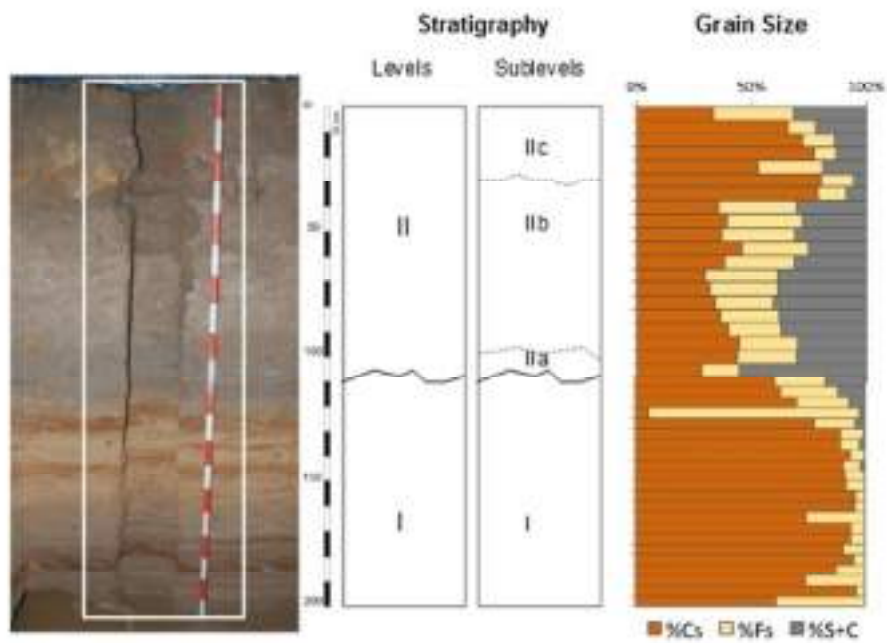


Figure 5. Stratigraphy and grain size distribution of sequence Ce3. (%Cs: percentage of coarse sand; %FS: percentage of fine sand; %S+C: percentage of silt and clay)
155x106mm (96 x 96 DPI)

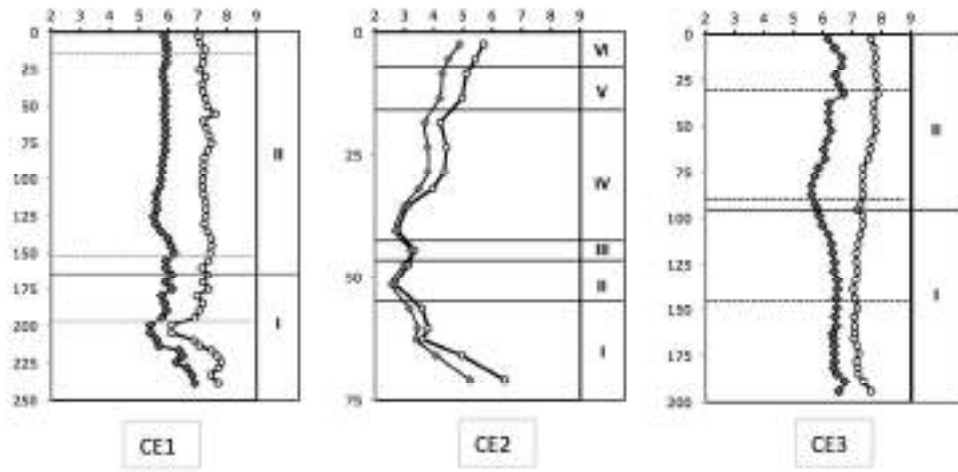


Figure 6. Soil reaction in sequences Ce1, Ce2 and Ce3. pH in KCl, black circles; pH in water, white circles.
161x84mm (300 x 300 DPI)

Peer Review

1
2
3
4
5
6
7
8
9
10
11
12
13
14
15
16
17
18
19
20
21
22
23
24
25
26
27
28
29
30
31
32
33
34
35
36
37
38
39
40
41
42
43
44
45
46
47
48
49
50
51
52
53
54
55
56
57
58
59
60

1
2
3
4
5
6
7
8
9
10
11
12
13
14
15
16
17
18
19
20
21
22
23
24
25
26
27
28
29
30
31
32
33
34
35
36
37
38
39
40
41
42
43
44
45
46
47
48
49
50
51
52
53
54
55
56
57
58
59
60

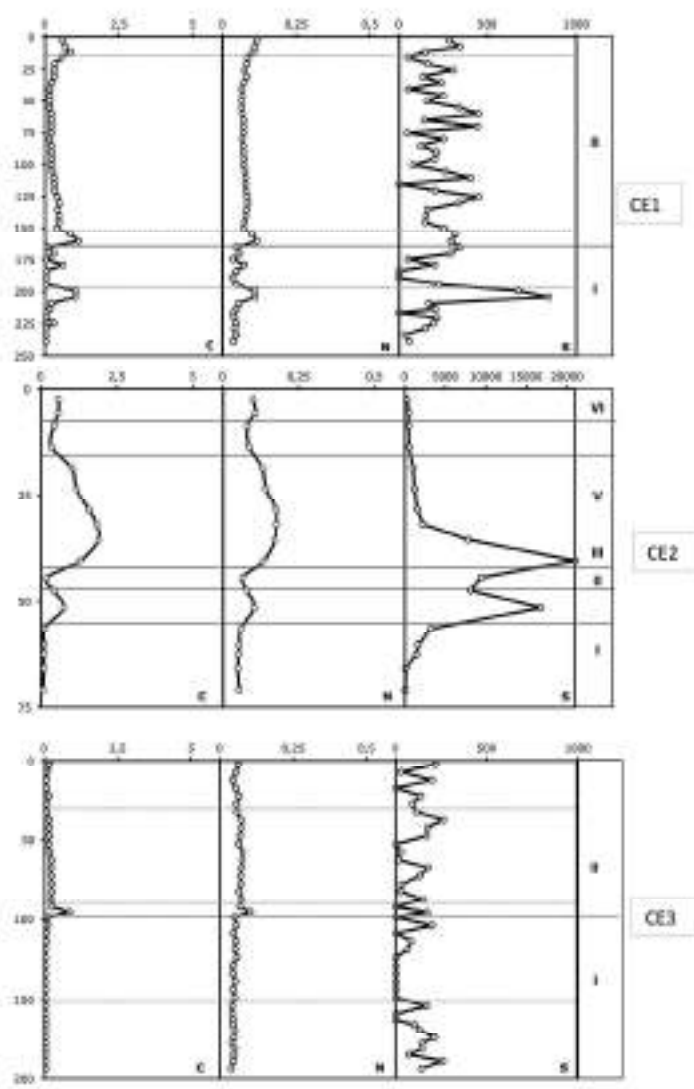


Figure 7. C (%), N (%) and S ($\mu\text{g g}^{-1}$) contents in sequences Ce1, Ce2 and Ce3
141x224mm (300 x 300 DPI)

1
2
3
4
5
6
7
8
9
10
11
12
13
14
15
16
17
18
19
20
21
22
23
24
25
26
27
28
29
30
31
32
33
34
35
36
37
38
39
40
41
42
43
44
45
46
47
48
49
50
51
52
53
54
55
56
57
58
59
60

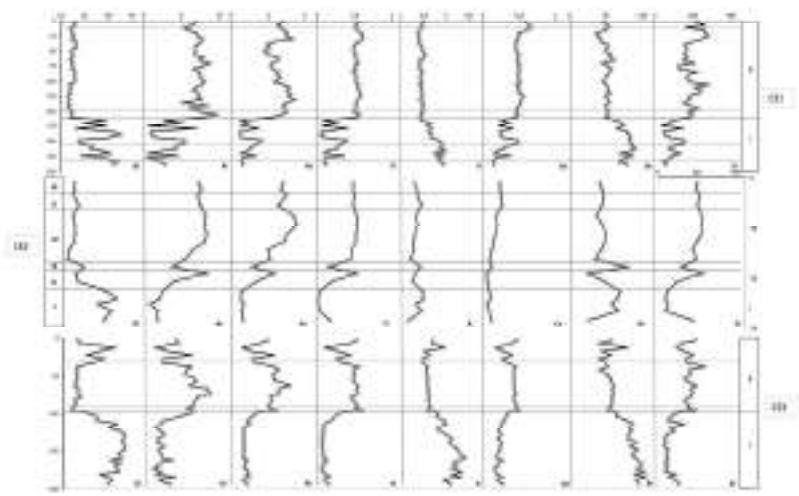


Figure 8. Content of Si (%), Al (%), Fe (%), Ti (%), K (%), Ca (%), Sr ($\mu\text{g g}^{-1}$) and Zr ($\mu\text{g g}^{-1}$) in Ce1, Ce2 and Ce3.
297x209mm (300 x 300 DPI)

Review

1
2
3
4
5
6
7
8
9
10
11
12
13
14
15
16
17
18
19
20
21
22
23
24
25
26
27
28
29
30
31
32
33
34
35
36
37
38
39
40
41
42
43
44
45
46
47
48
49
50
51
52
53
54
55
56
57
58
59
60



Figure 9. A reconstruction of shorelines from maps produced in 1880 and 1850 AD. 143x83mm (300 x 300 DPI)

er Review

1
2
3
4
5
6
7
8
9
10
11
12
13
14
15
16
17
18
19
20
21
22
23
24
25
26
27
28
29
30
31
32
33
34
35
36
37
38
39
40
41
42
43
44
45
46
47
48
49
50
51
52
53
54
55
56
57
58
59
60



Figure 10. Topography of the Vigo area taken from the IGN's (Spanish National Geographic Institute) 25 m DEM.
143x83mm (300 x 300 DPI)

1
2
3
4
5
6
7
8
9
10
11
12
13
14
15
16
17
18
19
20
21
22
23
24
25
26
27
28
29
30
31
32
33
34
35
36
37
38
39
40
41
42
43
44
45
46
47
48
49
50
51
52
53
54
55
56
57
58
59
60

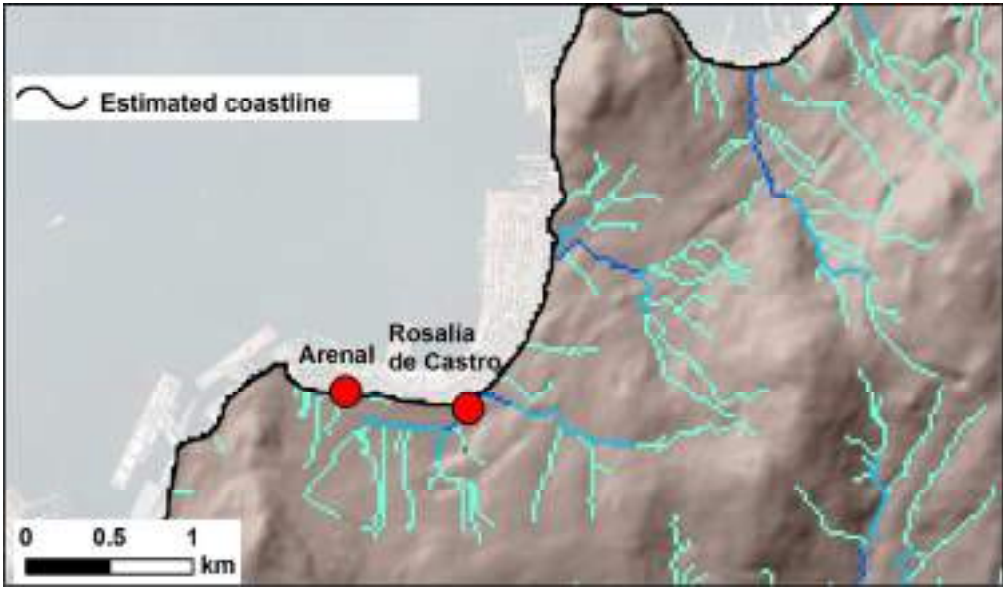


Figure 11. The potential drainage network calculated from a 25 m DEM 143x83mm (300 x 300 DPI)

er Review

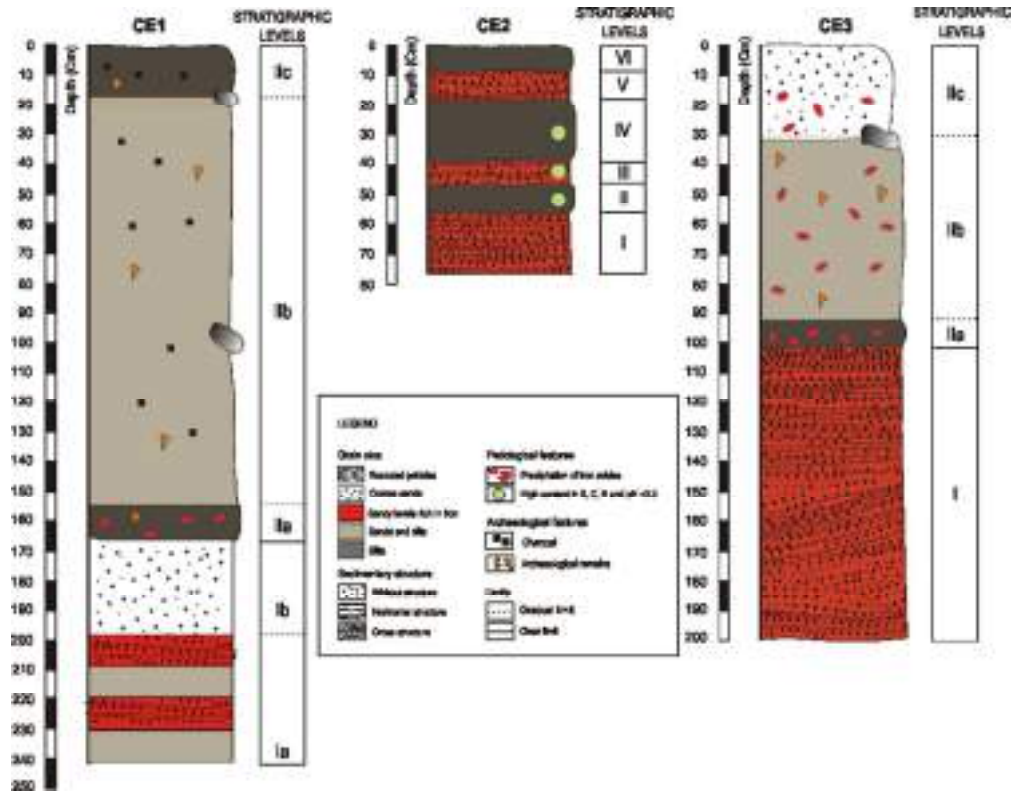


Figure 12. A stratigraphic synthesis of the pedo-sedimentary and archaeological features of Ce1, Ce2 and Ce3.
265x207mm (96 x 96 DPI)

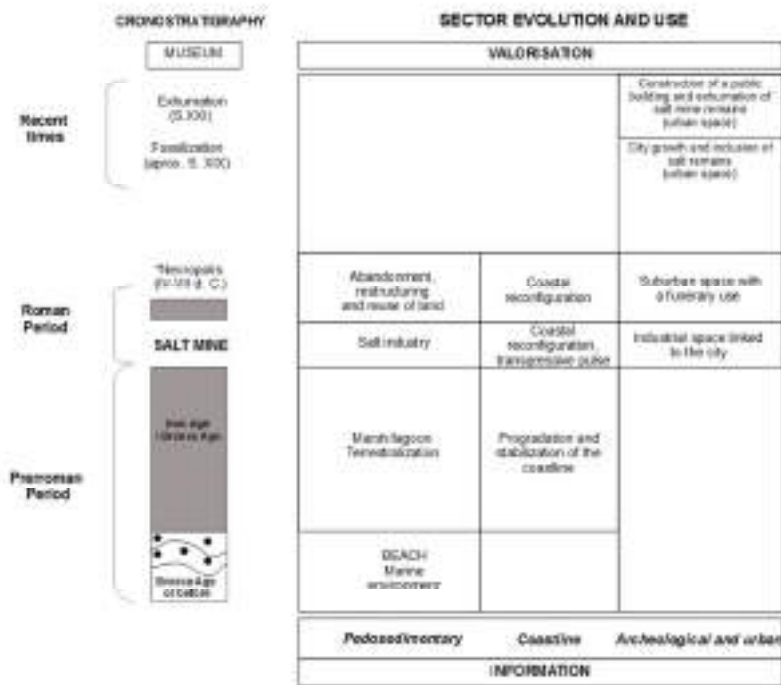


Figure 13. Chronostratigraphic reconstruction of the sequences studied 297x210mm (96 x 96 DPI)

Sample	Depth (cm)	Age ¹⁴ C BP	Age ¹⁴ C cal yr 2 sig BP	Age ¹⁴ C cal 2 sig BC/AD
Ce1-2	7,5	1740±40	1738-1541	220-400 AD
Ce1-8	35,5	2500±40	2739-2454	790-490 BC
Ce1-33	160,5	2950±40	3247-2975	1300-1020 BC
Ce1-42	204,5	3550±40	3928-3715	1980-1760 BC
Ce2-13	51,5	2700±40	2868-2749	920-800 BC
Ce3-20	95,75	3220±40	3490-3366	1540-1420 BC

For Peer Review

Fraction <2mm	Q	F	M	M-V	1:1	Gib
Ce1-1	xx	x	t	t	xxx	
Ce1-4	xx	x	t	t	xxx	
Ce1-7	x	x	x	t	xxx	t
Ce1-11	x	x	x	t	xxx	
Ce1-13	x	x	x	t	xxx	t
Ce1-16	x	x	x	t	xxx	t
Ce1-17	x	x	x	t	xxx	t
Ce1-19	xx	x	x	x	xxx	t
Ce1-21	xx	t	x	t	xxx	t
Ce1-25	xx	x	x	t	xxx	t
Ce1-27	xx	x	t	t	xxx	t
Ce1-29	x	x	x	t	xxx	
Ce1-31	xx	t	x	t	xxx	t
Ce1-33	xx	x	x	t	xxx	t
Ce1-34	xxx	t				
Ce1-37	xxx	x	x	t	xx	
Ce1-39	xxx	t				
Ce1-41	xxx	x	x	t	xx	
Ce1-43	xxx	x	t			t
Ce1-46	xxx	t				
Ce1-47	xxx	x	x	t	xx	
Ce1-50	xxx	t				
Ce2-2	t	t	x	t	xxx	
Ce2-4	t	t	x	t	xxx	
Ce2-6	t	t	x	t	xxx	
Ce2-8	t	t	x	x	xxx	
Ce2-9	x	t	t		xxx	
Ce2-11	xxx	x				
Ce2-12	x	t	x	x	xxx	t
Ce2-15	xxx	t				
Ce2-17	xxx	x				
Ce3-2	xx	x	x		xx	
Ce3-3	xxx	x	t			
Ce3-7	xxx	t	t			
Ce3-8	xx	x	x		xx	
Ce3-9	xx	t	x		xx	
Ce3-11	xx	t	x		xx	
Ce3-13	x	t	x		xx	
Ce3-16	x	t	t		xx	
Ce3-19	x	t	x		xx	
Ce3-20	x	t	x		xx	
Ce3-23	xxx	t				
Ce3-27	xxx	t				
Ce3-30	xxx	x	t			
Ce3-31	xxx	t				
Ce3-34	xxx	x	t			
Ce3-36	xxx	x	t			
Ce3-39	xxx	t				
Ce3-40	xxx	x	t			